HYDROSTATIC PRESSURE SENSOR BASED ON MODE INTERFERENCE OF A FEW MODE FIBER

D. Chen[1, 2, *], C. Wu[2], M.-L. V. Tse[2], and H. Y. Tam[2]

[1]Institute of Information Optics, Zhejiang Normal University, Jinhua 321004, China

[2]Photonics Research Centre, Department of Electrical Engineering, The Hong Kong Polytechnic University, Hung Hom, Kowloon, Hong Kong SAR, China

Abstract—A novel hydrostatic pressure sensor based on a few mode fiber (FMF) is proposed. The FMF-based hydrostatic pressure sensor is simply formed by splicing a segment of FMF to two segments of single mode fibers, where the FMF is used as the sensing element. The mode interference between LP_{01} mode and LP_{11} mode of the FMF provides an interference spectrum of the FMF-based hydrostatic pressure sensor which is sensitive to the hydrostatic pressure applied on the FMF. We experimentally show that there is a linear relationship between the hydrostatic pressure and the wavelength shift of the interference spectrum of the FMF-based hydrostatic pressure sensor.

1. INTRODUCTION

Optical fiber sensors which can measure a large range of physical, chemical and environmental variables such as temperature, pressure, position, displacement, chemical concentration, moisture, acceleration, load, flow and strain have attracted considerable attention in the past few decades due to their advantages such as small size, light weight, high sensitivity, multiplexing capability, immunity to electromagnetic interference and so on [1–17]. Among them, several techniques for optical fiber based hydrostatic pressure sensors have been proposed and demonstrated. In 1989, Bock and Domanski demonstrated a high hydrostatic pressure sensor based on the beat length measurement of

a highly birefringent optical fiber [18]. In 1991, dynamic pressure sensing was achieved based on an interferopolarimetric method [19]. In 1992, Wang et al. demonstrated a hydrostatic pressure sensor combining a special photoelastic material [20], where several non-optical fiber devices such as polarizers, quarter-wave-plates and GRIN lens ware used in the sensor head. In 1998, a side-hole optical fiber pressure sensor was proposed based on the measurement of the pressure-induced birefringence using a matched low-coherence interferometer [21]. More recently, several all-fiber hydrostatic pressure sensors such as hydrostatic pressure sensors based on all-fiber Sagnac interferometer [22], dual-core fiber [23], or fiber Bragg grating [24] have been proposed, which will be more suitable for applications in a harsh environment.

In this paper, we propose a kind of hydrostatic pressure sensor based on a FMF with an operational principle of the mode interference between LP_{01} mode and LP_{11} mode. Hydrostatic pressure sensing is achieved by measuring the wavelength shift of the interference spectrum of the FMF-based hydrostatic pressure sensor. A sensing range of about 40 MPa and a sensitivity of about -23.7 pm/MPa (blueshift) of the proposed hydrostatic pressure sensor are demonstrated. The proposed hydrostatic pressure sensor may be also used for air pressure sensing and have advantages of simple structure, low cost, ease of fabrication and so on.

2. FEW MODE FIBER

A FMF with an external diameter (fiber core diameter) of 145 μm (17.65 μm) is fabricated by ourselves. Our FMF can support three modes when the operational wavelength is 1550 nm. Figure 1 shows the cross-section of the FMF and LP_{01} mode profile, LP_{11} mode profile, and LP_{21} mode profile of the FMF when the operational wavelength is 1550 nm. Note that all mode profiles are based on the major electric field component of the x-polarized modes. We use a full-vector finite-element method (FEM) is to investigate the guided modes of the FMF. Figure 2 shows effective indices of the LP_{01} mode, LP_{11} mode, and LP_{21} mode of the FMF in a wavelength range from 1500 nm to 1600 nm. For LP_{21} mode, a cut-off wavelength of about 1560 nm is observed, which indicates the FMF can only support two modes when the wavelength is larger than 1560 nm. Our calculations also show the confinement loss and bending loss of LP_{21} mode are much larger than two other modes.
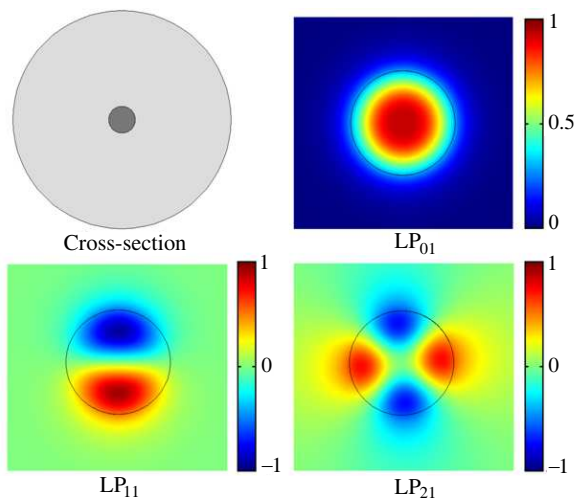
Figure 1. Cross-section and mode profiles (for LP_{01} mode, LP_{11} mode, and LP_{21} mode) of the FMF.
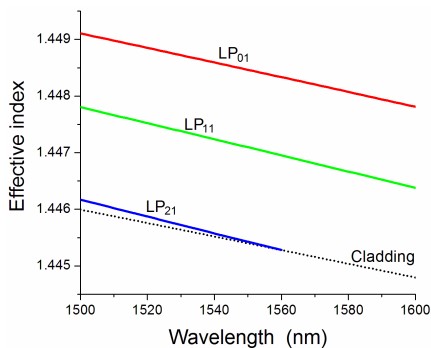
Figure 2. Effective index of LP_{01} mode, LP_{11} mode, and LP_{21} mode of the FMF.
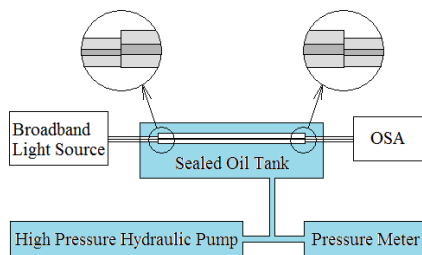
Figure 3. Schematic configuration of the hydrostatic pressure sensor and the test system.

3. HYDROSTATIC PRESSURE SENSOR

Figure 3 shows the schematic configuration of the proposed hydrostatic pressure sensor and the test system. A segment of 37-cm FMF (fabricated in The Hong Kong Polytechnic University) is spliced to two single mode fibers (SMFs) with an offset of about $10\,\mu m$ in the radial direction for each fusion-splicing point between the FMF and the SMF (to enhance the power of LP_{11} mode). An amplified spontaneous

emission (ASE) light source with an output spectrum from 1500 nm to 1600 nm is used as the broadband light source (BLS) in our experiment. An optical spectrum analyzer (OSA) with a resolution of 0.02 nm is used to detect the interference spectrum of the two modes of the FMF. The FMF is fixed inside a sealed oil tank. A high pressure hydraulic pump is used to control the hydrostatic pressure. The hydrostatic pressure is measured and displayed by a pressure meter.

When the light is injected into the FMF from the SMF, both LP_{01} mode and LP_{11} mode are excited in the FMF. The power will be dominantly distributed in LP_{01} mode and only a small portion of the power propagates in LP_{11} mode when the light is injected into central part of the FMF from the SMF. However, we can adjust the portion of the power propagates in the two modes by employing an offset in the radial direction between the FMF and the SMF which is controlled by a commercial fiber fusion splicer. In our experiment, the offset in the radial direction for the fusion-splicing point between the FMF and the SMF is about 10 μm, which efficiently enhances the power of LP_{11} mode. The two modes will interfere when the light recouples to the SMF, and the measured intensity can be given by [25]

$$I = I_1 + I_2 + 2\sqrt{I_1 I_2} \cos[2\pi \Delta n L/\lambda], \tag{1}$$

which is

$$I = 4I_0 \cos^2[\pi \Delta n L/\lambda], \tag{2}$$

When

$$I_1 = I_2 = I_0. \tag{3}$$

I_1 and I_2 are the power distributes in LP_{01} mode and LP_{11} mode inside the FMF, respectively. L is the length of the FMF and λ is the wavelength of the propagating light. $\Delta n = n_{01} - n_{11}$ is the mode index difference of LP_{01} mode (n_{01}) and LP_{11} mode (n_{11}), which is sensitive to the hydrostatic pressure applied on the FMF due to the photoelastic effect [24].

Figure 4 shows (a) the output spectrum (black dot dashed curve) of the BLS and output spectrum (red solid curve) of the hydrostatic pressure sensor and (b) transmission spectrum of the hydrostatic pressure sensor. The insert loss of the hydrostatic pressure sensor is about 10 dB, which is mainly due to the offset in the radial direction for the fusion-splicing point between the FMF and the SMF. The wavelength spacing of the interference spectrum (around 1550 nm) of the hydrostatic pressure sensor is about 8.9 nm, which is proportional to the length of the FMF. The extinction ratio is about 10 dB, which is enough for hydrostatic pressure sensing. The transmission spectrum of the hydrostatic pressure sensor is due to the interference of LP_{01} mode and LP_{11} mode which is described by the Eq. (1).
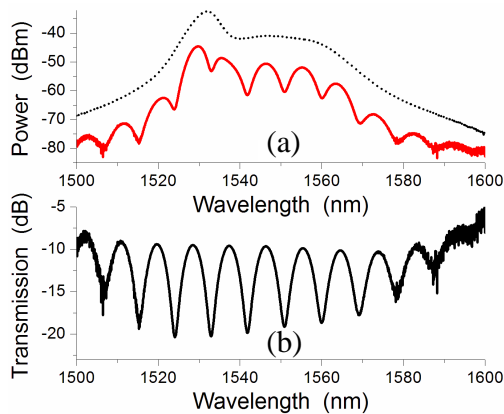
Figure 4. (a) Output spectrum (black dot dashed curve) of the broadband light source (BLS) and output spectrum (red solid curve) of the hydrostatic pressure sensor. (b) Transmission spectrum of the hydrostatic pressure sensor.

The hydrostatic pressure applied on the FMF-based hydrostatic pressure sensor is controlled by the high pressure hydraulic pump in the test system. When the pressure increases, the interference spectrum of the hydrostatic pressure sensor has a blue-shift. Figure 5(a) shows the blue-shift of wave trough (around 1550 nm) of the output spectrum of the hydrostatic pressure sensor when the applied pressure increases from 0 to 39 MPa. When we focus on the trough wavelength (around 1550 nm) of output spectrum of the hydrostatic pressure sensor, we can find a linear relationship between the hydrostatic pressure and wavelength shift of the interference spectrum of the hydrostatic pressure sensor, which is shown in Figure 5(b). In order to achieve more accurate information which the output spectrum of the hydrostatic pressure sensor carries, we achieve a polynomial expression by fitting a curve for the output spectrum. For example, we achieve the trough wavelength of the output spectrum by calculating the axis of symmetry of a second-order polynomial which is achieved by fitting the spectrum curve. The sensitivity ($S = \Delta\lambda/\Delta p$) of a pressure sensor is defined as the ratio of the wavelength change and the pressure change, which is about -23.7 pm/MPa (minus means a blueshift) for the proposed hydrostatic pressure sensor. The demonstrated measurement range of the hydrostatic pressure sensor is about 40 MPa, which is limited by our test system, but can be further improved for practical applications.
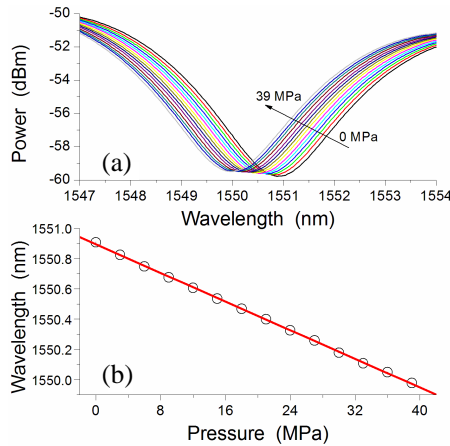
Figure 5. (a) Output spectra of the hydrostatic pressure sensor when the applied pressure increases from 0 to 39 MPa. (b) Wavelength shift of the trough wavelength (around 1550 nm) of the output spectra of the hydrostatic pressure sensor.

4. CONCLUSION

In conclusion, we have proposed and demonstrated a hydrostatic pressure sensor based on a FMF. We fabricated the FMF which can support 2 or 3 modes in the wavelength range from 1500 nm to 1600 nm. The FMF-based hydrostatic pressure sensor is simply formed by splicing a segment of FMF to two segments of SMFs. We have shown that the hydrostatic pressure applied on the FMF results in a blue-shift of the interference spectrum of the hydrostatic pressure sensor. The linear relationship between the hydrostatic pressure and the wavelength shift of the interference spectrum of the hydrostatic pressure sensor has been presented. A hydrostatic pressure sensor has been demonstrated with a sensitivity of -23.7 pm/MPa (blueshift) and a measurement range of about 40 MPa.

REFERENCES

1. Niklès, M., L. Thévenaz, and P. A. Robert, "Simple distributed fiber sensor based on Brillouin gain spectrum analysis," *Opt. Lett.*, Vol. 21, 758–760, 1996.

2. Kersey, A. D., M. A. Davis, H. J. Patrick, M. LeBlanc, K. P. Koo, C. G. Ashins, M. A. Putnam, and E. J. Friebele, "Fiber grating sensors," *J. Lightw. Technol.*, Vol. 15, 1442–1463, 1997.

3. Culshaw, B., "Optical fiber sensor technologies: Opportunities and-perhaps-pitfalls," *J. Lightw. Technol.*, Vol. 22, 39–50, 2004.

4. Farahani, M. A. and T. Gogolla, "Spontaneous raman scattering in optical fibers with modulated probe light for distributed temperature raman remote sensing," *J. Lightw. Technol.*, Vol. 17, 1379–1391, 1999.

5. Hill, K. O. and G. Meltz, "Fiber bragg grating technology fundamentals and overview," *J. Lightw. Technol.*, Vol. 5, 1263–1276, 1997.

6. Guan, B.-O., H.-Y. Tam, X.-M. Tao, and X.-Y. Dong, "Simultaneous strain and temperature measurement using a superstructure fiber Bragg grating," *IEEE Photon. Technol. Lett.*, Vol. 12, 675–677, 2000.

7. Liu, S. C., Z. W. Yin, L. Zhang, X. F. Chen, L. Gao, and J. C. Cheng, "Dual-wavelength FBG laser sensor based on photonic generation of radio frequency demodulation technique," *Journal of Electromagnetic Waves Applications*, Vol. 23, No. 16, 2177–2185, 2009.

8. Lu, H. H., C. H. Lee, K. P. Wen, C. H. Kuo, C. C. Liu, H. B. Wu, and J. S. Shin, "Direct-detection bidirectional radio-on-DWDM transport systems," *Journal of Electromagnetic Waves Applications*, Vol. 23, No. 7, 875–884, 2009.

9. Ni, J., B. Chen, S. L. Zheng, X. M. Zhang, X. F. Jin, and H. Chi, "Ultra-wideband bandpass filter with notched band based on electrooptic phase modulator and phase-shift fiber Bragg grating," *Journal of Electromagnetic Waves Applications*, Vol. 24, Nos. 5–6, 795–802, 2010.

10. Fu, X., C. Cui, and S. C. Chan, "Optically injected semiconductor laser for photonic microwave frequency mixing in radio-over-fiber," *Journal of Electromagnetic Waves Applications*, Vol. 24, No. 7, 849–860, 2010.

11. Liu, H.-Q., H.-C. So, K. W. K. Lui, and F. K. W. Chan, "Sensor selection for target tracking in sensor networks," *Progress In Electromagnetics Research*, Vol. 95, 267–282, 2009.

12. Chen, D., G. Hu, M. L. V. Tse, H. Y. Tam, and L. Gao, "Dual-core side-hole fiber for pressure sensing based on intensity detection," *Journal of Electromagnetic Waves Applications*, Vol. 25, Nos. 5–6, 775–784, 2011.

13. Ni, J., X. M. Zhang, S. L. Zheng, X. F. Jin, and H. Chi, "Microwave frequency measurement based on phase modulation to intensity modulation conversion using fiber Bragg grating," *Journal of Electromagnetic Waves Applications*, Vol. 25, Nos. 5–6, 755–764, 2011.

14. Chen, D., M.-L. V. Tse, C. Wu, G. Hu, and H.-Y. Tam, "Highly birefringent four-hole fiber for pressure sensing," *Progress In Electromagnetics Research*, Vol. 114, 145–158, 2011.

15. Wang, B., G. Somesfalean, L. Mei, H. Zhou, C. Yan, and S. He, "Detection of gas concentration by correlation spectroscopy using a multi-wavelength fiber laser," *Progress In Electromagnetics Research*, Vol. 114, 469–479, 2011.

16. Sun, N.-H., J.-J. Liau, Y.-W. Kiang, S.-C. Lin, R.-Y. Ro, J.-S. Chiang, and H.-W. Chang, "Numerical analysis of apodized fiber Bragg gratings using coupled mode theory," *Progress In Electromagnetics Research*, Vol. 99, 289–306, 2009.

17. He, M., J. Jiang, J. Han, and T. Liu, "An experiment research on extend range of based on fiber Bragg grating demodulation based on cwdm," *Progress In Electromagnetics Research Letters*, Vol. 6, 115–121, 2009.

18. Bock, W. J. and A. W. Domanski, "Highly hydrostatic pressure effects in highly birefringent optical fibers," *J. Lightw. Technol.*, Vol. 7, 1279–1283, 1989.

19. Charasse, M. N., M. Turpin, and J. P. Le Pesant, "Dynamic pressure sensing with a side-hole birefringent optical fiber," *Opt. Lett.*, Vol. 16, 1043–1045, 1991.

20. Wang, A., S. He, X. Fang, X. Jin, and J. Lin, "Optical fiber pressure sensor based on photoelasticity and its application," *J. Lightw. Technol.*, Vol. 10, 466–472, 1992.

21. Clowes, J. R., S. Syngellakis, and M. N. Zervas, "Pressure sensitivity of side-hole optical fiber sensors," *IEEE Photon. Technol. Lett.*, Vol. 10, 857–859, 1998.

22. Fu, H. Y., H. Y. Tam, L. Y. Shao, X. Dong, P. K. A. Wai, C. Lu, and S. K. Khijwania, "Pressure sensor realized with polarization-maintaining photonic crystal fiber-based Sagnac interferometer," *Appl. Opt.*, Vol. 47, 2835–2839, 2008.

23. Szczurowski, M. K., T. Martynkien, G. Statkiewicz-Barabach, W. Urbanczyk, and D. J. Webb, "Measurements of polarimentric sensitivity to hydrostatic pressure, strain and temperature in birefringent dual-core microstructured polymer fiber," *Opt. Express*, Vol. 18, 12076–12087, 2010.

24. Wu, C., B. O. Guan, Z. Wang, and X. Feng, "Characterization of pressure response of Bragg gratings in grapefruit microstructured fibers," *J. Lightw. Technol.*, Vol. 28, 1392–1397, 2010.

25. Liu, Y. and L. Wei, "Low-cost high-sensitivity strain and temperature sensing using graded-index multimode fibers," *Appl. Opt.*, Vol. 46, 2516–2519, 2007.